Rovibrational spectra of DCF$_3$ in the 1000 cm^{-1} region: The v_5 = 1 and v_6 = 2 levels revisited

Adina Ceausu-Velcescu [a,*], Petr Pracna [b], Adriana Predoi-Cross [c]

[a] Université de Perpignan, Laboratoire de Mathématiques, Physique et Systèmes, 52 Avenue Paul Alduy, 66860 Perpignan Cedex, France
[b] J. Heyrovský Institute of Physical Chemistry, v.v.i., Academy of Sciences of the Czech Republic, Dolejškova 3, 18223 Prague, Czech Republic
[c] University of Lethbridge, Department of Physics and Astronomy, 4401 University Drive, Lethbridge, AB, Canada T1 K 3M4

ABSTRACT

The degenerate fundamental vibrational level v_5 = 1 (975.51 cm^{-1}, E symmetry) and the overtone vibrational level v_6 = 2 (1004.06/1005.98 cm^{-1}, $A_1 + E$ symmetry) were reinvestigated with inclusion of their inter-vibrational couplings: the anharmonic Fermi interaction ($\Delta K = 0$, $\Sigma_t \Delta l_t = \Delta l_5 + \Delta l_6 = \pm 3$), the second-order Coriolis resonance ($\Delta K = \pm 1$, $\Sigma_t \Delta l_t = \pm 1$), and the second-order α-resonance ($\Delta K = \mp 2$, $\Sigma_t \Delta l_t = \pm 1$). This required significant extension of assignments to high J and K rotational states where resonant crossings due to the latter two interactions occur. The newly assigned data from Fourier-transform IR spectroscopy were combined with rotational and laser-sideband rovibrational data pertaining to the v_5 = 1 vibrational level, which were used already in a previous analysis, in a fully quantitative simultaneous fit.

© 2011 Elsevier Inc. All rights reserved.

1. Introduction

Although the first high-resolution study on the fundamental bands of DCF$_3$ was done already 25 years ago on the v_1 band [1], a systematic investigation by Fourier-transform IR and submillimeter wave spectroscopy of the remaining fundamental levels has been accomplished only during the last decade. The last fundamental level v_4 = 1 (degenerate CF$_3$ asymmetric stretching vibration) remained unanalyzed until very recently because of a complicated resonance system with the combination level $v_3 = v_6 = 1$ and a very congested spectrum of the two strong bands around 1200 cm^{-1} [2]. Except this case, all other fundamental levels of DCF$_3$ were studied as isolated vibrational levels because of seemingly sufficient separation from the neighboring levels. There remained, however, several unexplained anomalies which indicated that mutual interactions between the low-lying vibrational levels cannot be neglected.

In the case of the presently reinvestigated level v_5 = 1 (degenerate CD rock at 975 cm^{-1}) the analysis revealed the breakdown of the unitary equivalence of the Q- and D-reductions [3], which is considered to be a useful test of the validity of the isolated vibra-

tional level approximation. This breakdown was explained by the anomalous smallness of the effective q_{22} l-type interaction term [4] which can result from a neglected first-order Coriolis interaction with a nondegenerate vibrational level. The closest nondegenerate vibrational level v_2 = 1 (CF$_3$ symmetric stretching at 1111 cm^{-1}) was tested as a potential perturber, after having been analyzed in Ref. [5], with no success. Introducing the Coriolis coupling, estimated from the molecular force field [6], neither explained the small value of the q_{22} term in the v_5 = 1 level, nor the anomalous values of centrifugal distortion constants in the v_2 = 1 level [5]. This could not have been considered a final solution of the reduction breakdown problem because at that state of investigation the level closest to v_5 = 1, namely the v_6 = 2 level, was not analyzed yet.

The overtone level v_6 = 2 (the asymmetric CF$_3$ bending vibration) was first analyzed as an isolated vibrational level with the aim of determining the axial constants C_0, D_K^0, and eventually also H_K^0. This was done using the loop method combining the transitions of the fundamental v_6 band, the overtone band $v_6 = 2^{\pm 2} \leftarrow 0$ and the hot band $v_6 = 2^{\pm 2} \leftarrow 1^{\pm 1}$ [7]. The analysis of the v_6 = 2 level also disclosed the need of having the fundamental v_6 band [8] reassigned by interchanging the assignments of the $+l$ and $-l$ levels. This removed the disagreement of the reduction-dependent constants of the v_6 = 1 level of DCF$_3$ (η_J and η_K) with the force field calculations [6], which were otherwise in perfect agreement for the HCF$_3$ species. As this study used only rovibrational transitions with

low to moderate J and K-values, the $v_6 = 2$ overtone levels could still be considered as isolated. As a result, a very good reproduction of all the experimental data has been indeed achieved.

This first analysis of the $v_6 = 2$ level was an entry point to analyzing it with the inclusion of the vibration–rotation couplings to the $v_5 = 1$ level. It allowed us to estimate the positions of the resonant crossings between the two levels showing that they would occur for rotational levels with the K rotational number higher than in the former study [4]. This became a motivation for extending the assignments in both rovibrational bands and studying the effects of including these resonant couplings on the anomalies observed previously in vibrational states when studied as isolated ones.

2. Experimental details

Four high-resolution FTIR spectra were used in this work; one from the region of the v_6 band (spectrum I), used for assignments of the hot bands $v_6 = 2 \leftarrow 1$, and three spectra from the region of the v_5 and $2v_6$ bands (spectra IIa–c). The details of experimental conditions for all spectra are summarized in Table 1.

The spectra I and IIa and b, which were already used in Ref. [7], were recorded in Wuppertal with a Bruker IFS 120HR spectrometer. Spectra from the higher wavenumber region use the original calibration based on residual water lines taken from Ref. [9a] and corrected from systematic errors as indicated in Refs. [9b–9d]. Wavenumber precision and accuracy were 2×10^{-4} and 5×10^{-4} cm^{-1}, respectively. Spectrum I from the lower wavenumber region was calibrated by residual CO_2 lines from Ref. [9a]. As previously described, when combining spectra from two different regions, their simultaneous analysis may lead to a slight inconsistency of their absolute wavenumber calibration. It was removed by the same post-calibration of the spectrum I as used in Ref. [7]. As spectra IIa, b contain saturated lines for the lower J/K transitions, they were used mostly for extending assignments to higher values of J/K, both in the fundamental v_5 and overtone $2v_6^{\pm2}$ bands.

For assignments of the strong lines of the v_5 band we used spectrum IIc recorded at the Canadian Light Source in Saskatoon with a Bruker IFS 125HR spectrometer at considerably lower pressure and higher resolution. This spectrum was calibrated by well developed, isolated lines of CDF_3 from spectrum IIa in order to achieve the best wavenumber consistency of all three spectra from this region. Wavenumber precision and accuracy were estimated to be 1×10^{-4} and 3×10^{-4} cm^{-1}, respectively. A comparison of intensities and resolved spectral patterns in all three spectra IIa–c is shown in Fig. 1.

3. Theoretical model

The general $\mathbf{H}_{mn}$ notation, where m is the total power of vibrational operators and n the total power of rotational operators, has been used throughout the paper in the development of the rovibra-

Table 1
Experimental details of Fourier-transform spectra used in this study.

Spectrum	I	IIa	IIb	IIc
Range (cm^{-1})	400–880	850–1500	850–1500	800–1300
Detector	Cu:Ge	MCT800	MCT800	MCT800
Beamsplitter	KBr	KBr	KBr	KBr
No. of scans	340	80	360	472
Resolution [a] (cm^{-1})	0.0024	0.0024	0.0024	0.0015
Path length (m)	9.6	9.6	9.6	24
Pressure (Pa)	250	20	250	4
Temperature (K)	293	293	293	293

[a] The resolution of the Bruker FTS was calculated as 0.9/MOPD, where MOPD is maximum optical path difference.

tional Hamiltonian. Such a term is of order $i = m + n - 2$ in the Amat and Nielsen classification [10].

The effective Hamiltonians for the individual vibrational states $v_5 = 1$ and $v_6 = 2$ are essentially the same as in the studies in the approximation of isolated vibrational states expanded up to fifth order [4,7]. The matrix elements of these Hamiltonians are given in the Appendix A.

The additional part of the Hamiltonian which represents the interactions between the two levels includes an anharmonic Fermi interaction, a higher-order Coriolis resonance and a higher-order α-resonance. The explicit forms of all these terms up to fourth order, as well as those of their matrix elements, are given in the Appendix B. The notation of parameters closely follows that of Ref. [11].

With the use of the inter-vibrational interaction Hamiltonian the problem of its correct reduction arises. This means that a certain number of its parameters have to be constrained, corresponding to the number of free parameters of the contact transformation operators of the particular order of magnitude. The theory of reduction of the interaction Hamiltonian of this particular pair of vibrational levels $v_t = 1$ $(E)/v_{t'} = 2$ $(A_1 + E)$ is currently under investigation and we are using here some preliminary results [12] to determine the correct set of parameters for fitting our experimental data.

4. Results and discussion

4.1. Interactions between the $v_5 = 1$ and $v_6 = 2$ vibrational states

The situation of the $v_5 = 1$ and $v_6 = 2$ vibrational states is quite different from the previously studied case of the $v_4 = 1^{\pm1}$ and $v_3 = 1$, $v_6 = 1^{\pm1}$ vibrational states. The signs of the $C\zeta$ constants in the latter pair of interacting states together with the smaller separation of the levels led to resonant crossings of levels due to the anharmonic Fermi interaction, which occurred at intermediate values of K between 24 and 26 of the $l_4 = +1$ and $l_6 = +1$ sublevels. Besides this major resonance, we found resonant crossings involving levels differing in K by 1, . . ., 6.

In the present case the anharmonic Fermi interaction connects the $v_5 = 1^{\pm1}$ and $v_6 = 2^{\mp2}$ sublevels, i.e. with the non-vanishing matrix elements of the Hamiltonian obeying the selection rule $\Delta K = 0, \Sigma_t \Delta l_t = \Delta l_5 + \Delta l_6 = \pm3$. The separation of interacting levels can be estimated in the first approximation from the previously determined constants [4,7] as (in units of cm^{-1})

$$E_{vr}^5 - E_{vr}^{662} = (E_5 - E_{662}) - 2(C\zeta_5 + 2C\zeta_{66})K \cdot \Delta K + \Delta(C - B)_{566}K^2$$
$$\approx -30.542 + 0.291K \cdot \Delta K + 0.001184K^2 \quad (1)$$

where we used the notation $\Delta(C - B)_{566} = (C_5 - B_5) - (C_{662} - B_{662})$.

This means that the levels with $K \cdot \Delta K < 0$ diverge from each other, whereas the levels with $K \cdot \Delta K > 0$ come closer together with growing K.[1] The resonant crossing in the present case would occur only for $K > 80$ which is far beyond the range of observable transitions. In spite of that, the Fermi interaction turned out to be significant in the present analysis after inclusion of the resonant vibration–rotation terms and was thus included in the interaction Hamiltonian in the final step of the analysis.

The selection rules for the strongest vibration–rotation interactions correlate $\Sigma_t \Delta l_t = \pm1$ with $\Delta K = \pm 1$ or ∓2. The first case corresponds to a second-order Coriolis interaction, the second to a second-order α-resonance. A simple estimate of the separation of the interacting levels shows that the resonant crossings due to the weaker α-resonance occur for K between 20 and 30, while

---

[1] It is more convenient here to use the $K \cdot \Delta K$ quantity, where $K = |k|$ and
$$\Delta K = \begin{cases} +1 \text{ for the } l_5 = +1 \text{ and } l_6 = -2 \text{ levels} \\ -1 \text{ for the } l_5 = -1 \text{ and } l_6 = +2 \text{ levels} \end{cases}.$$
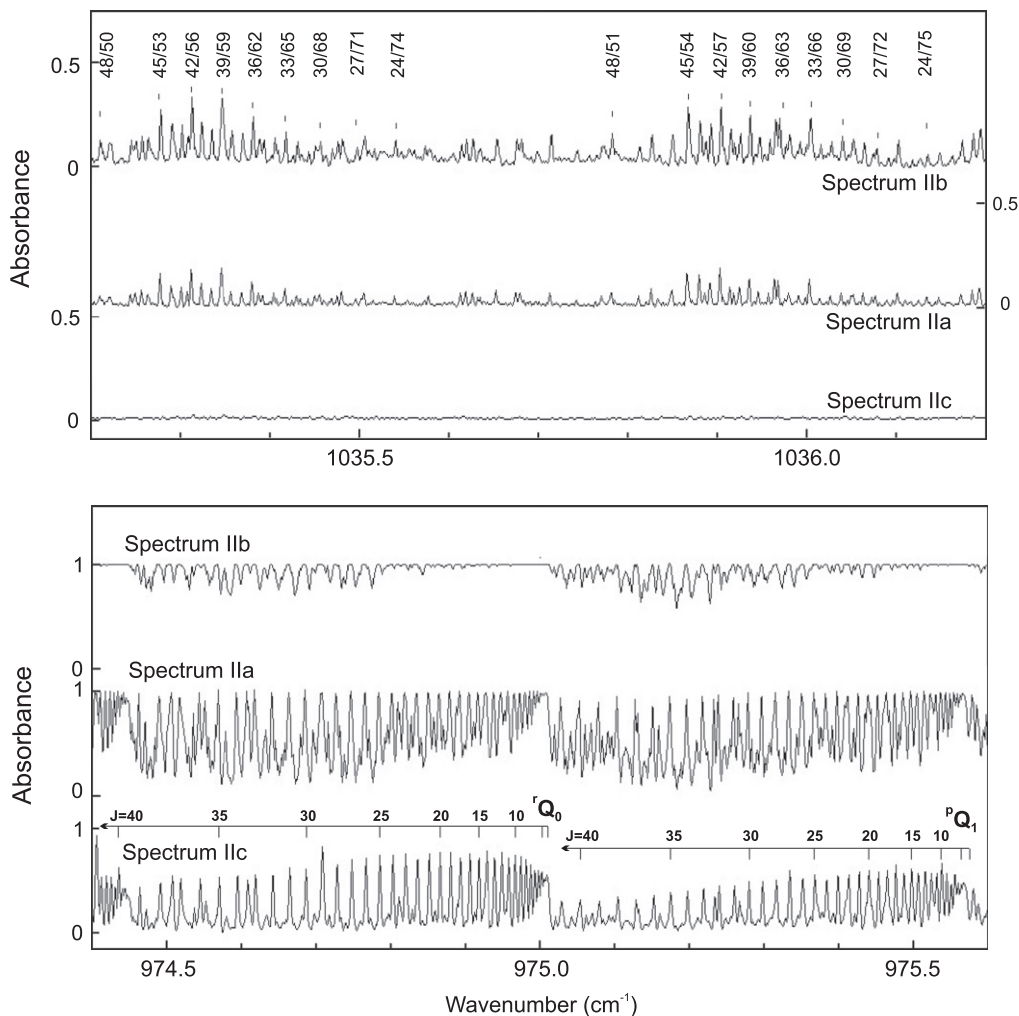
Fig. 1. Two sections of the Fourier-transform spectra showing pro-and-con's of different pressure/path length conditions. The strongest spectrum IIb provides extended assignments in the far wings of the v_5 band (upper frame with some K/J assignments in the ^{P}R branches indicated). The weakest spectrum IIc recorded with higher resolution provides well-resolved transitions at the band origin where the other two spectra IIa and IIb become saturated (lower frame).

those due to the Coriolis interaction occur only at $K \sim 50$. It is only the $v_5 = 1^{-1}$ sublevel which is involved in all possible vibration–rotation resonances because the $v_5 = 1^{+1}$ sublevel diverges from all sublevels of $v_6 = 2$.

The second-order α-resonance connects the pairs of levels $v_5 = 1^{-1}$, $K/v_6 = 2^{-2}$, $K + 2$. From the zero-order estimation of their separation (from constants of Refs. [4,7])

$$E_{vr}^5 - E_{vr}^{662} = [E_5 - E_{662} - 4(C_{662} - B_{662} + 2C\zeta_{66})] + 2(C\zeta_5$$
$$- 2C\zeta_{66} - 2(C_{662} - B_{662}))K + \Delta(C - B)_{566}K^2$$
$$\approx -28.840 + 1.413K + 0.001184K^2 \qquad (2)$$

it follows that the levels of the $v_5 = 1^{-1}$ sublevel up to $K = 20$ lie below those of the $v_6 = 2^{-2}$ sublevel as shown in Fig. 2 and no crossing occurs. Starting from $K = 21$ the relative position of these pairs is reversed and the crossing within the J-sequences occurs, subsequently between $J = 40/41$, 52/53, 60/61, 68/69, 74/75, ..., $K = 21$, ..., 25, ..., respectively. For $K \geqslant 25$ the crossings move beyond the range of observable transitions. The sequence of crossings occurs thanks to a combined effect of the difference of the B constants in these pairs ($B_{66} > B_5$) together with the effect of the q_{22} l-type interaction among the levels $v_6 = 2^{-2}$, $K - 2/2^0$, $K/2^{+2}$, $K + 2$ which pushes the levels of $v_6 = 2^{-2}$ up towards the $v_5 = 1^{-1}$ levels. This weaker α-resonance was not detected in the former study of the $v_5 = 1$ level [4] because only transitions with J

up to 50 were studied in the range of $K = 20$–30 (spectrum IIa) and the larger residuals in the J-series of $K = 21$ were not attributed to this resonance because the exact position of the $v_6 = 2$ level was not known at that time. This resonance had to be analyzed in detail before extensions of assignment to higher-K states and assessments of the stronger second-order Coriolis resonance.

Since the resonance pertains only to the $v_5 = 1^{-1}$, $K/v_6 = 2^{-2}$, K^{+2} pair of levels, the corresponding interaction constant $\tilde{f}_{32}^{xxb}$ does not suffer from correlations with other parameters once the data around the resonance crossings are assigned and fitted. The counterpart of this interaction connecting the pair of levels $v_5 = 1^{+1}$, $K/v_6 = 2^0$, $K + 2$ remains non-resonant as the levels stay separated in the whole range of studied data. The corresponding term $\tilde{f}_{32}^{xxa}$ is therefore correlated with other non-resonant terms in the Hamiltonian as will be described further. Therefore, we kept it constrained to a value close to that of the $\tilde{f}_{32}^{xxb}$ term in the earlier stages of the analyses and released it only in the final fits. It should be noted that the higher-order term $\tilde{f}_{32}^{xxb}$ had to be fitted before the larger, lower-order ones of the Fermi and Coriolis interactions. In these early stages of the analyses the values of the latter lower-order constants $k_{ta2t'a}$, $\tilde{f}_{31}^{xa}$, and $\tilde{f}_{31}^{xb}$ had to be constrained to zero which led to still effective values of the centrifugal distortion constants and did not allow for quantitative fitting of data for $K > 40$.
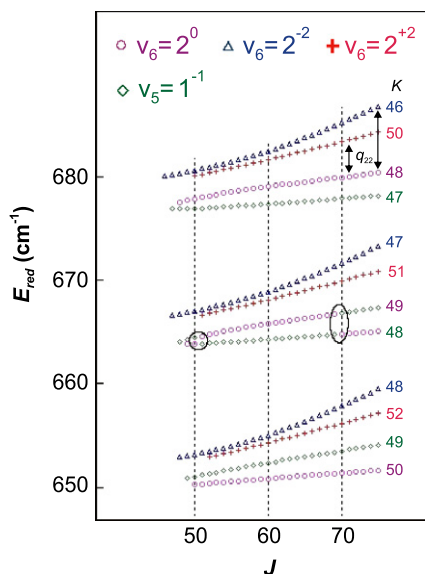
The second-order Coriolis interaction connects the $v_5 = 1^{-1}$ sublevel with two sublevels of the overtone level, i.e. $v_5 = 1^{-1}$,
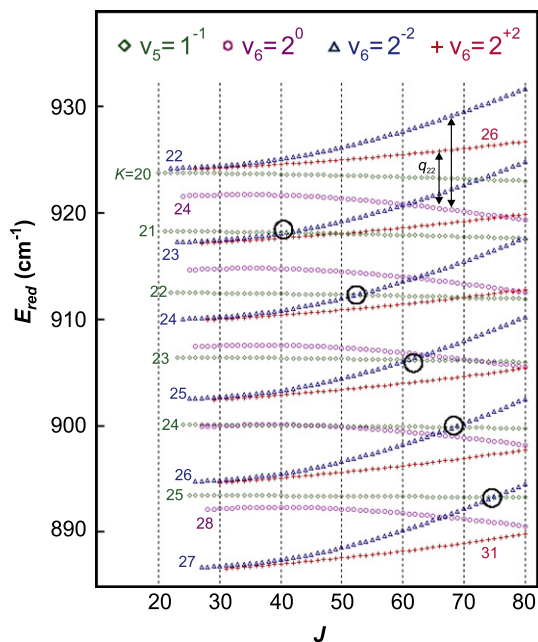
Fig. 2. J-reduced energy diagram $E_{\mathrm{red}} = E_{vr}(J,k,l) - B_0 J(J+1) + D_J^0 J^2 (J+1)^2 - H_J^0 J^3 (J+1)^3$ with indication of resonant level crossings due to the second-order α-resonance. The q_{22} interactions among the closely lying levels $v_6 = 2^0$ and $2^{\pm 2}$ are indicated with vertical arrows.

$K/v_6 = 2^0$, $K+1$ and $v_6 = 2^{-2}$, $K-1$. The crossing occurring at lower values of K is the one with the $v_6 = 2^0$ sublevel. After significant extensions of assignments of the high-K transitions in the $^P R_K$ branches for $K > 40$ and their fitting, the position of the crossing was refined to the pair $v_5 = 1^{-1}$, $K = 48/v_6 = 2^0$, $K = 49$ as shown in Fig. 3. We were indeed able to find the corresponding $^P R_{49}$ branch of the v_5 band and also several branches $^q X_K$ ($X = P/Q/R$, $K = 48–51$) of the $2v_6^0$ band with intensities enhanced by the resonance interaction and fit them in a satisfactory manner.

Using further refined parameters we were able to finally estimate the position of the second crossing to occur the first time for the pair $v_5 = 1^{-1}$, $K = 53/v_6 = 2^{-2}$, $K = 52$ and afterwards for several higher values of K, as shown in Fig. 4. The search for the cor-

responding branches in the vicinity of this resonance in either of the bands was not successful because the otherwise very useful interactive lower state combination difference (LSCD) checking method [13] was loosing its power with the rapidly vanishing line intensities and no apparent branch patterns were observable in the Loomis–Wood diagrams. We were able to assign tentatively only the $^P Q_{51}$ and $^P R_{51}$ branches of the v_5 band which have intensities enhanced by spin statistics but not any other transitions closer to the estimated resonance. Including these transitions to the $K = 50$ level of $v_5 = 1^{-1}$ in the fit had virtually no influence on the corresponding $\tilde{f}_{31}^{xb}$ Coriolis parameter (c.f. Eq. (B16) of Appendix B) and the $^P Q_{51}$ and $^P R_{51}$ branches remained poorly reproduced. This can be explained by the lack of data closer to the resonance, especially from the side of the $v_6 = 2^{-2}$ level where the assignments reach only $K = 42$. Therefore, we finally decided not to include the $^P Q_{51}$ and $^P R_{51}$ branches of the v_5 band into the fit.

4.2. Experimental data used in the analysis

For the investigation of the interactions between the $v_5 = 1$ and $v_6 = 2$ vibrational states we needed experimental data with an extension of their rotational states to significantly higher values of both J and K. We achieved that in the v_5 band by assigning transitions from spectrum IIb with the strongest absorption which enabled the extension of data across the several crossings due to the α-resonance and to the lower of the two crossings due to the Coriolis interaction. The weakest spectrum IIc recorded with a higher resolution, on the other hand, was used for assignments of low J and K transitions where the two spectra (IIa and b) recorded at higher pressures were saturated in the region close to the band origin. We collected finally over 10 000 newly assigned rovibrational transitions from these spectra, in contrast to about 1500 transitions used in the previous analysis [4].

The progress in the investigation of the $v_6 = 2$ vibrational level and making significantly extended assignments were enabled by resolving the α-resonance, first in the v_5 band. Consequently, we were able to assign transitions to the $v_6 = 2^{-2}$ sublevel in the region of the resonance for $K = 24–26$. Only after having this resonant interaction preliminarily fitted, it became possible to propagate
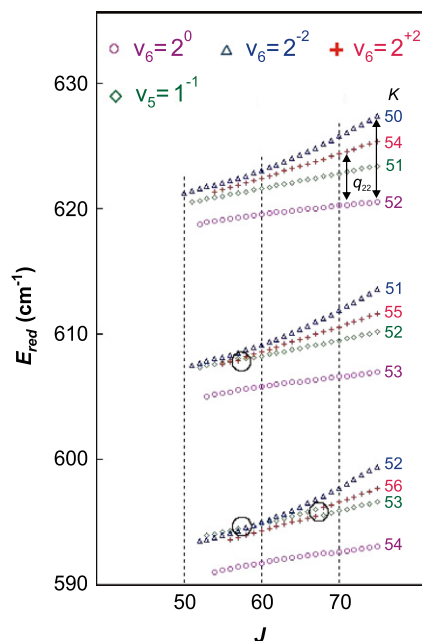

Fig. 3. J-reduced energy diagram with indication of resonant level crossings due to the second-order Coriolis interaction reached by assignments both in the v_5 and $2v_6^0$ bands.

Fig. 4. J-reduced energy diagram with indication of resonant level crossings due to the second-order Coriolis interaction which could not be assigned due to vanishing intensities.

the assignments to higher-K states, for which the weak transitions of the $v_6 = 2 \leftarrow 1$ hot bands are buried below much stronger transitions of the v_6 band and those of the $v_6 = 2^{\pm2} \leftarrow 0$ overtone band below the strong v_5 band. Finally we were able to assign several high-K branches in the weak $v_6 = 2^0 \leftarrow 0$ overtone band enhanced by intensity borrowing from the v_5 band in the neighborhood of the Coriolis resonant crossing. We also extended assignments of the perturbation allowed transitions with $\Delta K = \pm 3$ in the $v_6 = 2^{\pm2} \leftarrow 1^{\mp1}$ hot band having the origin in the strong mixing of the $(v_6 = 1^{+1}, k + 1/v_6 = 1^{-1}, k - 1)$ levels in the lower state of the hot band due to the q_{22} l-type resonance, as described in Ref. [7].

The infrared data were combined in a simultaneous analysis with much more accurate rotational and laser-sideband data which were used in the previous analysis of the v_5 band [4] to show their consistency with the new analysis. An overview of data used in the analysis is given in Table 2.

4.3. Reduction of the effective rovibrational Hamiltonian and fitting the data

Already in the very first stages of the analysis, the need to have two independent Coriolis parameters quickly became evident. In fact, with the two parameters dynamically constrained to a common (fitted) value, we were not able to reproduce the data with $K \geqslant 42$ of the $\Delta K = -1$ side of the v_5 band in a satisfactory manner. The convergence of the Hamiltonian was indeed very poor, even if we tried to introduce, besides the second-order Coriolis between v_5 and $2v_6$, the first-order Coriolis coupling between the $v_5 = 1$ level and the closest fundamental level of A_1 symmetry, $v_2 = 1$ lying about 136 cm^{-1} above.

The convergence of the Hamiltonian became significantly improved by fitting independently the $\tilde{f}_{31}^{xa}$ and $\tilde{f}_{31}^{xb}$ Coriolis parameters. Afterwards, we were also able to introduce the Fermi term $k_{ta2t'a}$. However, due to persisting correlations, it was not possible to refine it together with the Coriolis terms $\tilde{f}_{31}^{xa}$ and $\tilde{f}_{31}^{xb}$. Therefore, its value was first changed stepwise (and kept fixed) with the remaining interaction parameters refined. At this stage of the refinement, we also introduced in the fit the quadratic K-dependent terms of the Coriolis couplings, $\tilde{f}_{33}^{xa,K}$ and $\tilde{f}_{33}^{xb,K}$.

This procedure revealed a shallow minimum of the standard deviation of the fit for a value of $|k_{ta2t'a}| \approx 1.32$ cm^{-1}. After this preliminary setting of the interaction constants of the $\mathbf{H}_{30}$ and $\mathbf{H}_{31}$ Hamiltonians, when the reproduction of experimental data was better but still not satisfactory, we could start refining the higher-order expansion terms of the interaction Hamiltonian, starting with the J-dependent terms of $\tilde{f}_{31}^{xa}$ and $\tilde{f}_{31}^{xb}$ and then adding also the corresponding K-dependent terms. While we were able to refine the K-dependent term $\tilde{f}_{33}^{xa,K}$, the high correlations in the fit

when the $\tilde{f}_{33}^{xb,K}$ term was refined needed to constrain temporarily the $\tilde{f}_{33}^{xa,K}$ and also the $\tilde{f}_{32}^{xxa}$ and $\tilde{f}_{32}^{xxb}$ terms. These were further refined when the $\tilde{f}_{33}^{xb,K}$ term was constrained again.

With these terms refined, we repeated the refinement of the Fermi term which led to its increase to $|k_{ta2t'a}| \approx 1.44$ cm^{-1}. Because of strong correlations, we always had to constrain in further refinements of $k_{ta2t'a}$ the K-dependent terms of the Coriolis interactions. Such procedure of alternatively constraining and releasing parameters of the interaction Hamiltonian was found to be the only way how to avoid strong correlations but refine parameters which were significant for improving the reproduction of experimental data. However, we have to admit that the set of parameters suffering from such correlations, i.e. $k_{ta2t'a}, \tilde{f}_{32}^{xxa}$, and $\tilde{f}_{33}^{xb,K}$, still contains a certain degree of effectivity which we are unable to avoid.

Such correlations are a consequence of the limited set of experimental data that do not reach to the resonant crossings rather than due to an incorrect reduction of the interaction Hamiltonian. According to the reduction theory [12], there are four free parameters of the contact transformation of the interaction Hamiltonian up to order $\mathbf{H}_{32}$ which require constraining of four parameters of the effective interaction Hamiltonian. This is accomplished by constraining the parameters $f_{31}^z, k_{ta2t'a}^K, f_{32}^{xza}$, and f_{32}^{xzb}, leading to the set of free parameters which were varied in the present study.

In the least-squares fitting procedure, the data were given weights proportional to the inverse square of their estimated experimental uncertainties. Overlapped IR lines were given higher uncertainties based on the extent of discrepancy with the LSCD checks. Because of frequent overlaps of lines in the congested spectra, the fraction of lines with increased uncertainties is quite high. With this weighting we were able to reproduce all IR experimental data quantitatively, as summarized in Table 2. The only exception where the reproduction failed were the $^PQ_{51}$ and $^PR_{51}$ branches of the v_5 band which were excluded from the fit as mentioned above. We included in the simultaneous fit also the rotational data in the $v_5 = 1$ vibrational state and the IR laser-sideband data, both having an accuracy of about 50 kHz to show their consistency with the new analysis in a more general representation of interacting vibrational states. The purely rotational data were reproduced equally well as before, whereas the laser-sideband data, that pertain only to the lowest-K rotational levels ($K \leqslant 3$), have the standard deviation of reproduction 109 kHz, about twice as large as in the previous study [4].

The resulting parameters of the vibrational states $v_5 = 1$ and $v_6 = 2$ and the interaction terms are listed in Tables 3 and 4. In general, the parameters have lower standard errors than in the previous studies, thanks to the considerable extension of the data set. The centrifugal distortion constants are close to the ground state values, which indicates that no significant neglected terms would be effectively absorbed into their values. The small changes of

Table 2
Summary of experimental data for the $v_5 = 1$ and $v_6 = 2$ vibrational levels of DCF$_3$.

	Range of J/K	No. of data [a]	Estimated precision [b]	Standard deviation [b]
v_5	80/52	10 237	2	2.3
$2v_6^{\pm2}$	69/41	1823	2	2.9
$2v_6^0$	67/48–51	76	2	4.4
$2v_6^{\pm2} - v_6^{\pm1}$	70/50	1947	2	2.6
$2v_6^0 - v_6^{\pm1}$	56/45	1248	2	2.2
$2v_6^{\pm2} - v_6^{\mp1}$ PA[c]	51/42	556	2	2.1
$v_5 = 1$ rotational MMW [d]	22/18	172	50	54
$v_5 = 1$ laser-sideband [d]	34/3	124	50	109

[a] Total number of data with nonzero weights.
[b] In units of 10^{-4} cm^{-1} for IR data and kHz for rotational data.
[c] Perturbation-allowed transitions $\Delta K = \pm3$ (see text).
[d] Ref. [4].

Table 3
Molecular parameters of DCF$_3$ (in cm^{-1}) in the diagonal ground, $v_5 = 1$, and $v_6 = 2$ ($l = 0, \mp 2$) vibrational blocks.

Parameter	Ground state	$v_5 = 1$	$v_6 = 2, l = 0$	$v_6 = 2, l = \mp 2$
E	0	975.50827184(33)	1004.060259(26)	1005.983767(13)
B	0.3309331091	0.330621982(31)	0.33109428(10)	0.331060407(49)
C	0.18924413	0.189243975(22)	0.188516503(97)	0.188537132(64)
$D_J \times 10^7$	3.198603	3.21823(34)	3.26789(83)	3.24482(24)
$D_{JK} \times 10^7$	−4.89265	−4.80395(81)	−5.2268(20)	−5.03242(64)
$D_K \times 10^7$	2.1789	2.09656(58)	2.4372(19)	2.24021(82)
$H_J \times 10^{12}$	0.4745	0.4437(17)	0.4745[b]	0.4745[b]
$H_{JK} \times 10^{12}$	−2.0065	−1.972(16)	−2.330(58)	−2.477(18)
$H_{kJ} \times 10^{12}$	2.5994	3.371(22)	2.967(77)	2.954(35)
$H_K \times 10^{12}$	−1.0496	−2.265(14)	−1.0496[b]	−1.0496[b]
$C\zeta$		0.138488953(57)		−0.14155320(17)
$\eta_J \times 10^6$		1.64062(61)		−1.1250(10)
$\eta_K \times 10^6$		−1.56914(81)		0.8982(11)
$\tau_J \times 10^{12}$		−10.72(61)		
$\tau_{JK} \times 10^{10}$		2.1183(80)		
$\tau_K \times 10^{10}$		−2.3431(39)		
$q_{22} \times 10^4$		−0.198170(53)	−2.64097(98)	
$f_{22}^J \times 10^{10}$		9.095(28)	10.127(91)	
$f_{22}^K \times 10^{10}$		0	−10.07(12)	
$f_{42} \times 10^{10}$		−5.57(16)		
$d_t \times 10^7$		4.1804(76)		−1.088378[c]
$d_t^J \times 10^{12}$		2.6011[a]		
$h_3 \times 10^{14}$	−7.4939	−7.4939[b]		
$h_3^J \times 10^{19}$	4.77	4.77[b]		

Numbers in parentheses are standard deviations in units of the last digit quoted.
[a] Constrained to a value quoted in Ref. [4].
[b] Constrained to the corresponding ground state values.
[c] Constrained to the corresponding $v_6 = 1$ value, quoted in Ref. [7].

Table 4
Inter-vibrational interaction parameters for the $v_5 = 1/v_6 = 2$ level system of DCF$_3$ (in cm^{-1}).

Interaction	Parameter	Value
Coriolis ($\Delta k = \Sigma_t \Delta l_t = \pm 1$) $(v_5^{l_5} = 1^{\pm 1}, k \pm 1)/(v_6^{l_6} = 2^0, k)$	$f_{31}^{xa} \times 10^3$	−3.734 (33)
	$f_{33}^{xaJ} \times 10^7$	−3.55 (14)
	$f_{33}^{xa.K} \times 10^6$	5.345[a]
Coriolis ($\Delta k = \Sigma_t \Delta l_t = \pm 1$) $(v_5^{l_5} = 1^{\pm 1}, k)/(v_6^{l_6} = 2^{\pm 2}, k \pm 1)$	$f_{31}^{xb} \times 10^3$	−7.298 (30)
	$f_{33}^{xbJ} \times 10^7$	−8.18 (14)
	$f_{33}^{xb.K} \times 10^6$	1.044[a]
α-resonance ($\Delta k = \pm 2, \Sigma_t \Delta l_t = \mp 1$) $(v_5^{l_5} = 1^{\pm 1}, k)/(v_6^{l_6} = 2^0, k \pm 2)$	$f_{32}^{xxa} \times 10^5$	−3.28 (39)
α-resonance ($\Delta k = \pm 2, \Sigma_t \Delta l_t = \mp 1$) $(v_5^{l_5} = 1^{\pm 1}, k)/(v_6^{l_6} = 2^{\pm 2}, k \mp 2)$	$f_{32}^{xxb} \times 10^6$	9.556 (24)
Fermi ($\Delta k = 0, \Sigma_t \Delta l_t = \pm 3$)	$k_{ta2t'a}$	−1.442[a]

Numbers in parentheses are standard deviations in units of the last digit quoted.
[a] Constrained to a value obtained in a preliminary fit (see text).

values of the Hamiltonian parameters with respect to the previous studies [4,7] result from the inclusion of the inter-vibrational couplings, especially the anharmonic Fermi term. It should be noted, that the inclusion of interactions coupling the $v_5 = 1$ level to $v_6 = 2$ has not changed dramatically the anomalously small value of its q_{22} l-type constant, which means that the problem of breakdown of the D-reduction of the effective Hamiltonian in the $v_5 = 1$ level persists and that the Q-reduction should be used with preference. It was verified that this issue of reduction breakdown cannot be attributed to the neglected first-order Coriolis interaction between the $v_5 = 1$ level and $v_2 = 1$ fundamental levels. Testing of

the inclusion of this interaction into the current analysis neither showed any influence on the anomalous values of centrifugal distortion constants observed in the $v_2 = 1$ level [5]. Therefore, its source should be rather sought for in its Coriolis interaction with the $v_4 = 1$ level which also exhibits a similar anomaly of centrifugal distortion constants [2].

5. Conclusion

The current study presents a further step in the global understanding of the lowest vibrational levels of DCF$_3$ by investigation of the couplings between the closely lying levels $v_5 = 1$ and $v_6 = 2$, separated by approximately 30 cm^{-1}. The reproduction of the data extended significantly to high J and K rotational levels required the inclusion of the anharmonic Fermi, second-order Coriolis and α-resonance interactions. It demonstrates that the interaction with the closest fundamental level $v_2 = 1$ can be neglected and that the model of a dyad of interacting levels can be used for a fully quantitative reproduction of experimental data.

authors would like to thank the authors of Ref. [12] for communicating their results prior to publication.

Appendix A. Definition of matrix elements of the vibrational diagonal blocks in the effective vibration–rotation Hamiltonian

The diagonal matrix elements up to fifth order were taken as

$$
\begin{aligned}
E_{vr}(J,K,l) &= E_v + B_v J(J+1) + (C_v - B_v)K^2 - D_J^v J^2(J+1)^2 \\
&\quad - D_{JK}^v J(J+1)K^2 - D_K^v K^4 + H_J^v J^3(J+1)^3 \\
&\quad + H_{JK}^v J^2(J+1)^2 K^2 + H_{KJ}^v J(J+1)K^4 + H_K^v K^6 \\
&\quad + [-2C\zeta_v + \eta_J^v J(J+1) + \eta_K^v K^2 + \tau_J^v J^2(J+1)^2 \\
&\quad + \tau_{JK}^v J(J+1)K^2 + \tau_K^v K^4]Kl
\end{aligned}
\tag{A1}
$$

The diagonal z-Coriolis term $C\zeta_v$ (and its expansion η and τ – terms) vanish for the ground vibrational state. For the definition of Hamiltonian off-diagonal matrix elements, it is more appropriate to use the signed quantum number k ($K = |k|$), because they can in general connect rotational states with different signs of k.

In the $v_5 = 1$ and $v_6 = 2$ vibrational levels the following l-type operators were taken into account

$$
\begin{aligned}
&\langle v_t^{l_t \pm 2}; J, k \pm 2 | \mathbf{H}_{22} + \mathbf{H}_{24} | v_t^{l_t}; J, k \rangle \\
&= [(v_t \mp l_t)(v_t \pm l_t + 2)]^{1/2} \{ q_{22} + f_{22}^J J(J+1) + f_{22}^K [k^2 \\
&\quad + (k \pm 2)^2] \} F_2^\pm(J,k)
\end{aligned}
\tag{A2}
$$

$$
\langle v_t^{l_t \pm 2}; J, k \mp 4 | \mathbf{H}_{24} | v_t^{l_t}; J, k \rangle = [(v_t \mp l_t)(v_t \pm l_t + 2)]^{1/2} f_{42} F_4^\mp(J,k)
\tag{A3}
$$

Because of the accidental smallness of the q_{22} term in the $v_5 = 1$ level we used the effective Hamiltonian in the Q-reduction (with the constraint $q_{12}^5 = 0$). In the $v_6 = 2$ vibrational level there was not such a problem and the two reductions Q and D were equivalent. We thus used the Q-reduction in both studied levels with the matrix elements of the operator describing the $\Delta k = \pm 3$ interaction in the form

$$
\langle v_t^{l_t}; J, k \pm 3 | \mathbf{H}_{23} + \mathbf{H}_{25} | v_t^{l_t}; J, k \rangle = [d_t + d_t^J J(J+1)]l_t F_3^\pm(J,k)
\tag{A4}
$$

The matrix elements of the operator of the $\Delta k = \pm 6$ interaction

$$
\langle v_t^{l_t}; J, k \pm 6 | \mathbf{H}_{06} + \mathbf{H}_{08} | v_t^{l_t}; J, k \rangle = [h_3 + h_3^J J(J+1)]F_6^\pm(J,k)
\tag{A5}
$$

were included in the vibrational ground state and in the $v_5 = 1$ level.

The notation of the matrix elements of rotational shifting operators was taken conventionally as

$$
F_n^\pm(J,k) = \prod_{i=1}^n [J(J+1) - (k \pm i \mp 1)(k \pm i)]^{1/2}
\tag{A6}
$$

Appendix B. Definition of matrix elements of the interaction block in the effective vibration–rotation Hamiltonian

The inter–vibrational interaction Hamiltonian was considered here up to fourth order: $\mathbf{H}_{int} = \mathbf{H}_{30} + \mathbf{H}_{31} + \mathbf{H}_{32} + \mathbf{H}_{33}$.

The interaction Hamiltonians and the corresponding off-diagonal matrix elements are given in the equations below, where $t = 5$ and $t' = 6$. The ladder operators J_σ ($\sigma = \pm 1$) and $L_{t\varepsilon}^\sigma$ ($\sigma, \varepsilon = \pm 1$, the two signs are independent) are those used in Ref. [11], whose actions are the following

$$
J_\sigma |J,k\rangle = [J(J+1) - k(k-\sigma)]^{1/2}|J, k - \sigma\rangle
\tag{B1}
$$

$$
L_{t\varepsilon}^\sigma |v_t, l_t\rangle = [(v_t + \sigma + 1 + \sigma\varepsilon l_t)/2]^{1/2}|v_t + \sigma, l_t + \varepsilon\rangle
\tag{B2}
$$

The Fermi interaction between the $v_5 = 1$ and $v_6 = 2$ levels was described by the following Hamiltonians

$$
\mathbf{H}_{30} = \frac{3}{4} k_{ta2t'a} \{ (L_{t'-}^- L_{t'-}^- L_{t-}^+ + L_{t'+}^- L_{t'+}^- L_{t+}^+) + (L_{t'+}^+ L_{t'+}^+ L_{t+}^- + L_{t'-}^+ L_{t'-}^+ L_{t-}^-) \}
\tag{B3}
$$

$$
\mathbf{H}_{31}^z = f_{31}^z \{ (L_{t'-}^- L_{t'-}^- L_{t-}^+ - L_{t'+}^- L_{t'+}^- L_{t+}^+)J_z + (L_{t'+}^+ L_{t'+}^+ L_{t+}^- - L_{t'-}^+ L_{t'-}^+ L_{t-}^-)J_z \}
\tag{B4}
$$

$$
\begin{aligned}
\mathbf{H}_{32}^J + \mathbf{H}_{32}^K &= \frac{3}{4} \{ (L_{t'-}^- L_{t'-}^- L_{t-}^+ + L_{t'+}^- L_{t'+}^- L_{t+}^+) + (L_{t'+}^+ L_{t'+}^+ L_{t+}^- \\
&\quad + L_{t'-}^+ L_{t'-}^+ L_{t-}^-) \} (k_{ta2t'a}^J J^2 + k_{ta2t'a}^K J_z^2)
\end{aligned}
\tag{B5}
$$

with the corresponding matrix elements

$$
\begin{aligned}
&\left\langle v_t^{l_t} = 1^{\mp 1}, v_{t'} = 0; J, k \middle| \mathbf{H}_{30} + \mathbf{H}_{32}^J + \mathbf{H}_{32}^K \middle| v_t = 0, v_{t'}^{l_{t'}} = 2^{\pm 2}; J, k \right\rangle \\
&= \frac{3}{4}\sqrt{2}[k_{ta2t'a} + k_{ta2t'a}^J J(J+1) + k_{ta2t'a}^K k^2]
\end{aligned}
\tag{B6}
$$

$$
\left\langle v_t^{l_t} = 1^{\mp 1}, v_{t'} = 0; J, k \middle| \mathbf{H}_{31}^z \middle| v_t = 0, v_{t'}^{l_{t'}} = 2^{\pm 2}; J, k \right\rangle = \pm k\sqrt{2}f_{31}^z
\tag{B7}
$$

The second-order Coriolis interaction ($\Delta k = \sum_t \Delta l_t = \pm 1$) between the $v_5 = 1$ and $v_6 = 2$ levels was described by the Hamiltonians

$$
\mathbf{H}_{31}^{xa} = f_{31}^{xa} \{ L_{t'+}^- L_{t'-}^- (L_{t+}^+ J_- - L_{t-}^+ J_+) + L_{t'-}^+ L_{t'+}^+ (L_{t-}^- J_+ - L_{t+}^- J_-) \}
\tag{B8}
$$

$$
\mathbf{H}_{31}^{xb} = f_{31}^{xb} \{ (L_{t'+}^- L_{t'+}^- L_{t}^+ J_- - L_{t-}^- L_{t'-}^- L_{t+}^+ J_+) + (L_{t'-}^+ L_{t'-}^+ L_{t+}^- J_+ - L_{t'+}^+ L_{t'+}^+ L_{t-}^- J_-) \}
\tag{B9}
$$

$$
\begin{aligned}
\mathbf{H}_{32}^{xza} &= f_{32}^{xza} \{ L_{t'+}^- L_{t'-}^- (L_{t+}^+ [J_z, J_-]_+ + L_{t-}^+ [J_z, J_+]_+) \\
&\quad + L_{t'-}^+ L_{t'+}^+ (L_{t-}^- [J_+, J_z]_+ + L_{t+}^- [J_-, J_z]_+) \}
\end{aligned}
\tag{B10}
$$

$$
\begin{aligned}
\mathbf{H}_{32}^{xzb} &= f_{32}^{xzb} \{ (L_{t'+}^- L_{t'+}^- L_{t-}^+ [J_z, J_-]_+ + L_{t'-}^- L_{t'-}^- L_{t+}^+ [J_z, J_+]_+) \\
&\quad + (L_{t'-}^+ L_{t'-}^+ L_{t+}^- [J_+, J_z]_+ + L_{t'+}^+ L_{t'+}^+ L_{t-}^- [J_-, J_z]_+) \}
\end{aligned}
\tag{B11}
$$

$$
\begin{aligned}
\mathbf{H}_{33}^{xa,J} + \mathbf{H}_{33}^{xa,K} &= f_{33}^{xa,J} \mathbf{J}^2 \{ L_{t'+}^- L_{t'-}^- (L_{t+}^+ J_- - L_{t-}^+ J_+) + L_{t'-}^+ L_{t'+}^+ (L_{t-}^- J_+ - L_{t+}^- J_-) \} \\
&\quad + f_{33}^{xa,K} \{ L_{t'+}^- L_{t'-}^- (L_{t+}^+ [J_z^2, J_-]_+ - L_{t-}^+ [J_z^2, J_+]_+) \\
&\quad + L_{t'-}^+ L_{t'+}^+ (L_{t-}^- [J_z^2, J_+]_+ - L_{t+}^- [J_z^2, J_-]_+) \}
\end{aligned}
\tag{B12}
$$

$$
\begin{aligned}
\mathbf{H}_{33}^{xb,J} + \mathbf{H}_{33}^{xb,K} &= f_{33}^{xb,J} \mathbf{J}^2 \{ (L_{t'+}^- L_{t'+}^- L_t^+ J_- - L_{t'-}^- L_{t'-}^- L_{t+}^+ J_+) \\
&\quad + (L_{t'-}^+ L_{t'-}^+ L_{t-}^- J_+ - L_{t'+}^+ L_{t'+}^+ L_t^- J_-) \} \\
&\quad + f_{33}^{xb,K} \{ (L_{t'+}^- L_{t'+}^- L_{t-}^+ [J_z^2, J_-]_+ - L_{t'-}^- L_{t'-}^- L_{t+}^+ [J_z^2, J_+]_+) \\
&\quad + (L_{t'-}^+ L_{t'-}^+ L_{t+}^- [J_z^2, J_+]_+ - L_{t'+}^+ L_{t'+}^+ L_{t-}^- [J_z^2, J_-]_+) \}
\end{aligned}
\tag{B13}
$$

with the following matrix elements

$$
\begin{aligned}
&\left\langle v_t^{l_t} = 1^{\pm 1}, v_{t'} = 0; \ J, k \pm 1 \middle| \mathbf{H}_{31}^{xa} + \mathbf{H}_{33}^{xa,J} + \mathbf{H}_{33}^{xa,K} \middle| v_t = 0, v_{t'}^{l_{t'}} = 2^0; \ J, k \right\rangle \\
&= \pm \{ f_{31}^{xa} + f_{33}^{xa,J} J(J+1) + f_{33}^{xa,K} [k^2 + (k \pm 1)^2] \} F_1^\pm(J,k)
\end{aligned}
\tag{B14}
$$

$$
\begin{aligned}
&\left\langle v_t^{l_t} = 1^{\pm 1}, v_{t'} = 0; \ J, k \pm 1 \middle| \mathbf{H}_{32}^{xza} \middle| v_t = 0, v_{t'}^{l_{t'}} = 2^0; \ J, k \right\rangle \\
&= f_{32}^{xza}(2k \pm 1)F_1^\pm(J,k)
\end{aligned}
\tag{B15}
$$

$$
\begin{aligned}
&\left\langle v_t^{l_t} = 1^{\mp 1}, v_{t'} = 0; \ J, k \pm 1 \middle| \mathbf{H}_{31}^{xb} + \mathbf{H}_{33}^{xb,J} + \mathbf{H}_{33}^{xb,K} \middle| v_t = 0, v_{t'}^{l_{t'}} = 2^{\mp 2}; \ J, k \right\rangle \\
&= \pm \sqrt{2} \{ f_{31}^{xb} + f_{33}^{xb,J} J(J+1) + f_{33}^{xb,K} [k^2 + (k \pm 1)^2] \} F_1^\pm(J,k)
\end{aligned}
\tag{B16}
$$

$$\left\langle v_t^{l_t} = 1^{\mp 1}, v_{t'} = 0; J, k \pm 1 \left| \mathbf{H}_{32}^{xzb} \right| v_t = 0, v_{t'}^{l_{t'}} = 2^{\mp 2}; J, k \right\rangle$$
$$= \sqrt{2} f_{32}^{xzb} (2k \pm 1) F_1^{\pm}(J, k) \tag{B17}$$

The α-type interaction ($\Delta k = \pm 2, \sum_t \Delta l = \pm 1$) between the $v_5 = 1$ and $v_6 = 2$ levels was described by the following Hamiltonians

$$H_{32}^{xxa} = f_{32}^{xxa} \{ L_{t'+}^- L_{t'-}^- (L_{t+}^+ J_+^2 + L_t^+ J_-^2) + L_{t'-}^+ L_{t'+}^+ (L_{t-}^- J_-^2 + L_{t+}^- J_+^2) \} \tag{B18}$$

$$H_{32}^{xxb} = f_{32}^{xxb} \{ (L_{t'+}^- L_{t'+}^- L_{t}^+ J_+^2 + L_{t'-}^- L_{t'-}^- L_{t+}^+ J_-^2) + (L_{t'-}^+ L_{t'-}^+ L_{t+}^- J_-^2 + L_{t'+}^+ L_{t'+}^+ L_t^- J_+^2) \} \tag{B19}$$

with the corresponding matrix elements

$$\left\langle v_t^{l_t} = 1^{\pm 1}, v_{t'} = 0; J, k \mp 2 \left| \mathbf{H}_{32}^{xxa} \right| v_t = 0, v_{t'}^{l_{t'}} = 2^0; J, k \right\rangle$$
$$= f_{32}^{xxa} F_2^{\mp}(J, k) \tag{B20}$$

$$\left\langle v_t^{l_t} = 1^{\mp 1}, v_{t'} = 0; J, k \mp 2 \left| \mathbf{H}_{32}^{xxb} \right| v_t = 0, v_{t'}^{l_{t'}} = 2^{\mp 2}; J, k \right\rangle$$
$$= \sqrt{2} f_{32}^{xxb} F_2^{\mp}(J, k) \tag{B21}$$

Appendix C. Supplementary material

Supplementary data for this article are available on ScienceDirect (www.sciencedirect.com), as part of the Ohio State University Molecular Spectroscopy Archives (http://msa.lib.ohiostate.edu/jmsa_hp.htm), and in the online version. Supplementary data associated with this article can be found, in the online version, at doi:10.1016/j.jms.2011.03.016.

References

[1] H.-R. Dübal, M. Lewerenz, M. Quack, J. Chem. Phys. 85 (1986) 34–39.
[2] P. Pracna, A. Ceausu-Velcescu, A. Predoi-Cross, Š. Urban, J. Mol. Spectrosc. 259 (2010) 1–10, doi:10.1016/ j.jms.2009.09.007.
[3] J.K.G. Watson, C. Gerke, H. Harder, K. Sarka, J. Mol. Spectrosc. 187 (1998) 131–141.
[4] P. Pracna, K. Sarka, J. Demaison, J. Cosléou, F. Herlemont, M. Khelkhal, H. Fichoux, D. Papoušek, M. Paplewski, H. Bürger, J. Mol. Spectrosc. 184 (1997) 93–105.
[5] P. Pracna, Š. Urban, F. Kolář, J. Cosléou, J. Demaison, P. Paplewski, H. Bürger, J. Mol. Struct. 517–518 (2000) 119–126.
[6] J. Breidung, J. Cosléou, J. Demaison, K. Sarka, W. Thiel, Mol. Phys. 102 (2004) 1827–1841.
[7] P. Pracna, A. Ceausu-Velcescu, H. Bürger, J. Mol. Spectrosc. 250 (2008) 59–69, doi:10.1016/ j.jms.2008.04.011.
[8] H. Bürger, J. Cosléou, J. Demaison, C. Gerke, H. Harder, H. Mäder, M. Paplewski, D. Papoušek, K. Sarka, J.K.G. Watson, J. Mol. Spectrosc. 182 (1997) 34–49.
[9] (a) G. Guelachvili, K. Narahari Rao, Handbook of Infrared Standards, Academic Press, San Diego, 1986;
(b) G. Guelachvili, M. Birk, Ch.J. Bordé, J.W. Brault, L.R. Brown, B. Carli, A.R.H. Cole, K.M. Evenson, A. Fayt, D. Hausamann, J.W.C. Johns, J. Kauppinen, Q. Kou, A.G. Maki, K. Narahari Rao, R.A. Toth, W. Urban, A. Valentin, J. Vergès, G. Wagner, M.H. Wappelhorst, J.S. Wells, B.P. Winnewisser, M. Winnewisser, Pure Appl. Chem. 68 (1996) 193–208;
(c) G. Guelachvili, M. Birk, Ch.J. Bordé, J.W. Brault, L.R. Brown, B. Carli, A.R.H. Cole, K.M. Evenson, A. Fayt, D. Hausamann, J.W.C. Johns, J. Kauppinen, Q. Kou, A.G. Maki, K. Narahari Rao, R.A. Toth, W. Urban, A. Valentin, J. Vergès, G. Wagner, M.H. Wappelhorst, J.S. Wells, B.P. Winnewisser, M. Winnewisser, J. Mol. Spectrosc. 177 (1996) 164–179;
(d) G. Guelachvili, M. Birk, Ch.J. Bordé, J.W. Brault, L.R. Brown, B. Carli, A.R.H. Cole, K.M. Evenson, A. Fayt, D. Hausamann, J.W.C. Johns, J. Kauppinen, Q. Kou, A.G. Maki, K. Narahari Rao, R.A. Toth, W. Urban, A. Valentin, J. Vergès, G. Wagner, M.H. Wappelhorst, J.S. Wells, B.P. Winnewisser, M. Winnewisser, Spectrochim. Acta A 52A (1996) 717–732.
[10] G. Amat, H.H. Nielsen, J. Chem. Phys. 36 (1962) 1859–1865.
[11] K. Sarka, L. Nová Stříteská, J. Mol. Spectrosc. 257 (2009) 108–110, doi:10.1016/ j.jms.2009.06.006.
[12] K. Sarka, L. Nová Stříteská, private communication.
[13] W. Lodyga, M. Kreglewski, P. Pracna, Š. Urban, J. Mol. Spectrosc. 243 (2007) 182–188, doi:10.1016/j.jms.2007.02.004.